Nuclear quadrupole resonance of an electronically excited state from high-resolution hole-burning spectroscopy

Robert Klieber, Andreas Michalowski, Rudolf Neuhaus,* and Dieter Suter
Universität Dortmund, Fachbereich Physik, 44221 Dortmund, Germany
(Received 21 November 2002; revised manuscript received 7 March 2003; published 5 May 2003)

Hole-burning spectroscopy can eliminate inhomogeneous broadening and thereby resolve the fine structure of optical transitions. In the case of rare-earth ions at low temperatures, the homogeneous linewidth is often small compared to the splittings due to nuclear-spin interactions. Hole-burning spectra can then be used to measure, e.g., nuclear quadrupole couplings. We have used this technique to study the hyperfine interaction of Pr in Pr^{3+}:$YAlO_3$ in the electronic ground state as well as in an electronically excited state. Using a stabilized ring dye laser system (linewidth <30 kHz), we obtained hole-burning spectra that clearly resolved the excited-state interactions also. We show that the spectra depend sensitively on the relative orientation of the nuclear-spin quantization axes of the two electronic states. This allows us to decide between different values for the tensor orientation that have been published before.

DOI: 10.1103/PhysRevB.67.184103 PACS number(s): 32.70.Cs, 32.10.Fn

I. INTRODUCTION

Various nonlinear techniques have been developed to obtain optical spectra with a resolution that is not limited by the inhomogeneous linewidth. A relatively simple technique is hole burning, where a pump-laser beam modifies the populations of a subset of atoms or molecules that are in resonance with the narrowband pump.[1] A second laser beam, whose frequency can be tuned around the pump-laser frequency, probes the modified atoms and measures deviations from the thermal equilibrium absorption whenever the difference between pump- and probe laser frequency matches an internal energy difference; more precisely, the difference between pump and probe laser has to be equal to the sum or difference of two internal energy differences of the sample.

This technique has been applied, e.g., to measure nuclear-spin transitions in rare-earth crystals.[2,3] The population modifications introduced in this spectroscopic technique also form a basis for applications of these materials in optical storage[2] and signal processing.[4]

Experiments like these provide information about the energy-level structure and the populations of nuclear spin states. It is possible to measure the nuclear-spin-lattice relaxation time T_1.[5] Recently, photongated hole burning[6] has been observed in Pr:YAG and the mechanism was assigned to selective photoionization, which can also be obtained from photongated photoconductivity.[7] Cone showed[8] that hole-burning techniques in combination with the Raman spectroscopy can also be used to investigate defect sites and quadrupole splitting parameters of rare-earth compounds.

The resolution of the hole-burning spectra is limited by the stability of the laser sources. Commercial laser systems, which have linewidths of the order of 1 MHz, are therefore not suitable for measuring splitting frequencies of the same order of magnitude. We therefore added a laser frequency stabilization, which reduced the linewidth to ≈ 30 kHz. The resulting spectra show very well-resolved resonance lines that can be used to determine effective nuclear quadrupole coupling constants for both electronic states. Since the optical transition matrix elements depend sensitively on the overlap of the nuclear-spin states,[9,10] the relative orientation of the quantization axes between ground and electronically excited state is an important parameter for the calculation of the hyperfine-resolved spectra.

Several authors have already attempted to measure the (relative) orientation of the principal-axis systems of Pr^{3+}:$YAlO_3$. Wokaun *et al.*[11] obtained an angle of $\pm 16.5°$ from anticrossing experiments. Four years later Mitsunaga *et al.*[9] measured an angle of $\pm 12.8°$ by Raman spectroscopy. Stimulated photon echo experiments[12,13] indicated an angle of 40–60°, and coherent Raman beat experiments[14] lead to a value of $47 \pm 5°$.

The paper is structured as follows. In Sec. II, we calculate the hole-burning spectrum of Pr^{3+}:$YAlO_3$. The experimental section summarizes the laser stabilization scheme required to resolve the rather small excited-state interaction. The experimental results presented in Sec. IV allow us to measure the coupling strengths in both the electronic states and to determine the relative orientation of the principal-axis systems of both the states. The paper concludes with a summary of the main results.

II. THEORY

A. Energy-level structure

The orthorhombic unit cell of Pr^{3+}:$YAlO_3$ contains two inequivalent praseodymium sites with point symmetry C_{1h}. The electronic degeneracy of the $^3H_4$ ground state is completely removed by the crystal field; the separation between the lowest state (Γ_1) and the next-higher state (Γ_2) is $E_1 = 51\ \mathrm{cm}^{-1}$, corresponding to a temperature of $E_1/k_B = 73$ K. All transitions between levels of the same $4f^N$ configuration are weakly allowed for trivalent rare-earth ions in C_{1h} crystal fields,[15] and a long lifetime of the excited state ($T_1 = 180\ \mu$s[3,10]) leads to narrow homogeneous optical linewidth of ≈ 10 kHz at low temperatures. In this work, we consider the transition between the $^3H_4$ ground state and the $^1D_2$ excited state, which is centered at a wavelength of 610.69 nm.

The interaction between the nuclear spin $I = \frac{5}{2}$ of ^{141}Pr and the electric-field gradient tensor, as well as the second-

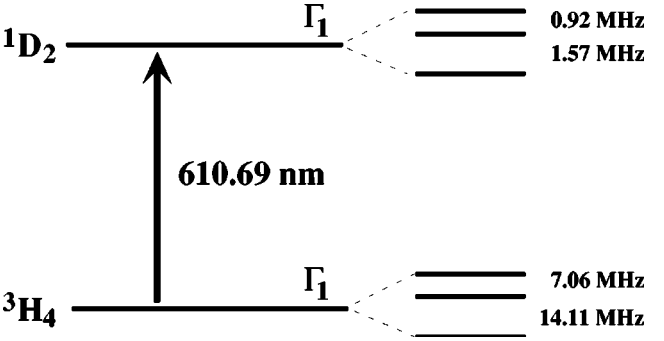

FIG. 1. Relevant part of the energy-level scheme of Pr^{3+}:$YAlO_3$. The hyperfine structure of the ground and the electronically excited states contain three doubly degenerate nuclear-spin substates.

order hyperfine interaction are best described as an effective quadrupole coupling that partially lifts the degeneracy of the nuclear-spin states.[16–19] The relevant nuclear-spin Hamiltonian, written in the principal-axis system of the effective quadrupole coupling, is

$$H_Q = D[I_z^2 - \tfrac{1}{3}I(I+1)] + E(I_x^2 - I_y^2). \tag{1}$$

The coupling constants D and E have been determined for the ground state $^3H_4$ ($D/h = -3.5289$ MHz, $E/h = -0.0118$ MHz), as well as for the excited state $^1D_2$ ($D/h = -0.4024$ MHz, $E/h = -0.0512$ MHz).[20–22] Since quadrupole coupling is negative, the state with the magnetic quantum number $\pm 5/2$ is the lowest ground level. The resulting hyperfine splittings between the three doubly degenerate pairs of substates are of the order 0.9, 1.6, and 2.5 MHz for the excited state and 7.1, 14.1, and 21.1 MHz for the ground state.[23] The relevant part of the energy-level scheme for the transition between $^3H_4$ and $^1D_2$ substates of Pr^{3+}:$YAlO_3$ is shown in Fig. 1.

The optical transition matrix elements μ_{ge} between the ground state $|g\rangle$ and the excited state $|e\rangle$ can be separated into the electronic part μ_{opt}, which is the same for all optical transitions, and the overlap integral of the nuclear wave functions $|\chi\rangle$:[10]

$$\mu_{ge} = \langle g|\mu\cdot\mathbf{E}|e\rangle = \langle\psi_g|\mu\cdot\mathbf{E}|\psi_e\rangle\langle\chi_g|\ \chi_e\rangle = \mu_{\mathrm{opt}}\langle\chi_g|\ \chi_e\rangle, \tag{2}$$

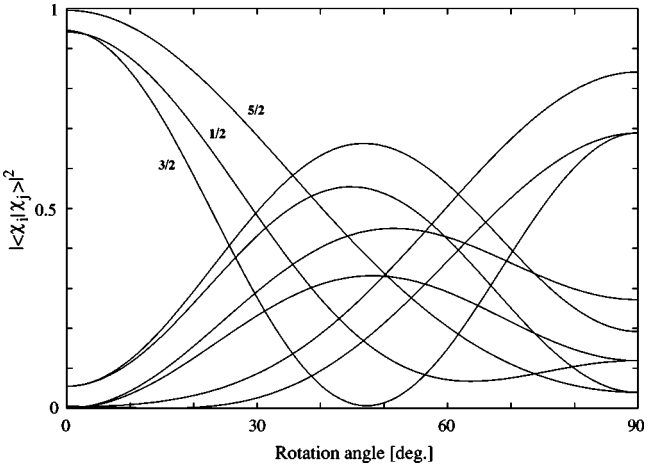

FIG. 2. Relative transition strengths between the ground and the excited states as a function of the rotation angle between the principal axes of both the states. Transitions between states with the same nuclear-spin quantum numbers are numbered in the figure.

where $|\psi\rangle$ describes the electronic part of the wave functions. The overlap integral of the nuclear wave functions $\langle\chi_g|\chi_e\rangle$ depends on the relative orientation of the quadrupole tensor axes of the ground vs the excited state.[9] Figure 2 shows the absolute squares of the overlap integrals for the nine transitions as a function of the rotation angle between the two principal axis systems.

B. Pump-laser field

We describe the effect of the pump-laser field on the populations with a generic model system that consists of three nuclear-spin states of the electronic ground state and a single substate of the electronically excited state. The pump-laser beam drives the transition from the ground state $|1\rangle$ to the excited state $|4\rangle$. The model neglects transfer of populations between the nuclear-spin substates of the electronically excited states, which is justified by the significantly longer nuclear-spin relaxation times compared to the electronic lifetime of the excited state. It also neglects transfer of populations into other excited or crystal field states. Since we do not consider coherent effects, a rate equation model is sufficient to describe the population dynamics:

$$\frac{d}{dt}\begin{pmatrix}\rho_{11}\\ \rho_{22}\\ \rho_{33}\\ \rho_{44}\end{pmatrix} = 2|\langle\chi_1|\chi_4\rangle|^2\left(\frac{\mu_{\mathrm{opt}}E}{2\hbar}\right)^2 T_2\begin{pmatrix}-1&0&0&1\\ 0&0&0&0\\ 0&0&0&0\\ 1&0&0&-1\end{pmatrix}\begin{pmatrix}\rho_{11}\\ \rho_{22}\\ \rho_{33}\\ \rho_{44}\end{pmatrix}$$
$$+\begin{pmatrix}-(\Gamma_{12}+\Gamma_{13})&\Gamma_{12}&\Gamma_{13}&\Gamma_{41}\\ \Gamma_{12}&-(\Gamma_{12}+\Gamma_{23})&\Gamma_{23}&\Gamma_{42}\\ \Gamma_{13}&\Gamma_{23}&-(\Gamma_{13}+\Gamma_{23})&\Gamma_{43}\\ 0&0&0&-1/T_1\end{pmatrix}\begin{pmatrix}\rho_{11}\\ \rho_{22}\\ \rho_{33}\\ \rho_{44}\end{pmatrix}. \tag{3}$$

The first term describes the transfer of population between states $|1\rangle$ and $|4\rangle$ by the laser field. The transfer rate is proportional to the square of the optical Rabi frequency for this transition and to the transverse relaxation time T_2 of the optical coherence, which was measured for Pr^{3+}:$YAlO_3$ as 78 μs.[24] The model neglects thus the effect of off-resonant irradiation.

The second term describes the effect of relaxation: the first three rows and columns describe the spin relaxation between the nuclear-spin substates of the ground state, while the fourth column is the spontaneous decay from the excited state. In the high-temperature approximation, the nuclear-spin relaxation rates are symmetric, $\Gamma_{ij}=\Gamma_{ji}; i,j=1 \ldots 3$. The optical decay rates Γ_{4i} are determined by the overlap integral

$$\Gamma_{4,g(g=1-3)}=\frac{|\langle\chi_4|\chi_g\rangle|^2}{T_1} \tag{4}$$

and therefore depend on the relative orientation of the two principal-axis systems.

C. Hole spectrum

A probe laser field with frequency ω_2, which is scanned through the absorption line, detects the modified populations through the change in optical absorption. A change occurs when the resonance condition is fulfilled, i.e., when the difference $(\omega_2-\omega_1)$ between the pump and the probe laser frequencies matches a sum or difference between two nuclear-spin transition frequencies (including zero).

The absorption change $\Delta A(\omega_2-\omega_1)$ can be approximated by

$$\Delta A(\omega_2-\omega_1)=|\langle\chi_{e'}|\chi_{g'}\rangle|^2(\rho_{g'g'}-\tfrac{1}{3})L(\Delta\omega). \tag{5}$$

The states $|g'\rangle$ and $|e'\rangle$ are coupled by the probe laser beam, and ω_0 is the resonance frequency of the transition $|g'\rangle\leftrightarrow|e'\rangle$. The lineshape function $L(\Delta\omega)$ turned out to be well approximated by a Lorentzian.

The hole-burning spectrum is obtained by calculating the equilibrium populations $\rho_{g'g'}$ for each of the nine pump configurations $(g,\ e=1 \ldots 3)$ and then letting the probe laser measure the deviations from the thermal equilibrium according to Eq. 5. Figure 3 shows, as an example, one such subspectrum, calculated for the pump configuration, shown in the inset, where the pump-laser beam drives the transition from the lowest ground state to the lowest excited state. The holes near $\omega_2=\omega_1$ correspond to those transitions where the probe laser connects the excited states to the lowest ground state (whose population is reduced), while the antiholes near -14 and -21 MHz correspond to the probe laser coupling the $\pm 3/2$ and $\pm 1/2$ ground states to the excited-state sublevels.

For each pump configuration, the probe laser can be resonant with nine different transitions, resulting in a total of 81 distinguishable ways of coupling the two laser fields to the atomic system. Since the frequencies of several transitions coincide (e.g., nine configurations where $\omega_1=\omega_2$), the hole spectrum contains 49 distinguishable resonance lines.

III. EXPERIMENTAL

A. Setup

The praseodymium doped crystal with the dimensions $5\times5\times1$ mm^3 was cooled to 5 K in a helium flow cryostat. We used a typical cw pump-probe configuration, with probe and pump beam crossing in the sample. Both linearly polarized laser beams (1 mm diameter) propagated roughly along the crystallographic c axis, intersecting at an angle of 5.7°. The pump laser beam was blocked behind the sample, whereas the probe beam was measured with a photodiode (New Focus 1804).

Pump and probe beams were derived from the same tunable, actively stabilized ring dye laser (Coherent 899−21). The frequencies of the two laser beams were shifted independently with two acousto-optic modulators (AOM's) by a retroreflection setup. The frequency of the pump beam was fixed while the probe laser frequency was swept linearly (using a direct digital synthesizer) by ± 46 MHz around the pump-laser frequency within 25 ms.

The intensity of the pump and probe laser was 127 W/m^2 and 63 W/m^2, respectively. At this temperature and pump-laser intensity, the spectral holes are close to their maximal values; a further increase of the pump power mainly results in line broadening. While the probe laser intensity was not much smaller than that of the pump laser, it did not significantly affect the populations, since it was scanned rapidly and therefore did not interact with any subset of atoms long enough to change their populations.

B. Laser stabilization

The width of the resonance lines in the hole-burning spectra is determined by the natural width of the optical resonance lines and by the frequency stability of the laser: not only the frequency jumps of the pump-laser beam cause wider holes, the probe laser frequency jitter also adds to the observed hole width. If hole-burning spectra are measured

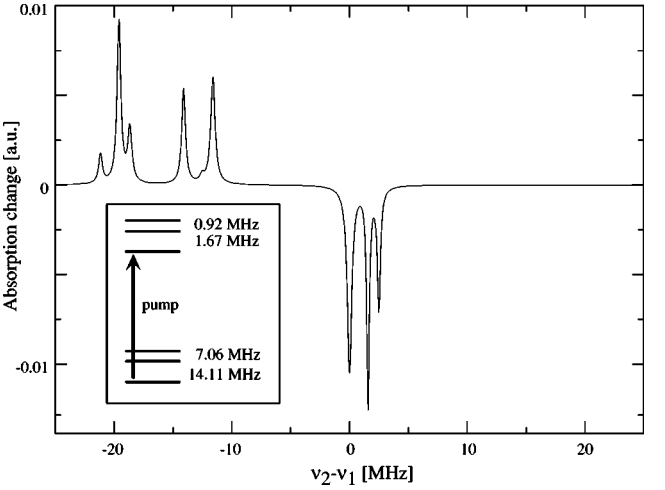

FIG. 3. Theoretical hole-burning spectrum for one of the nine pump configurations in Pr^{3+}:$YAlO_3$ at 5 K. The pump-laser beam drives the transition from the lowest ground state to the lowest excited state as shown in the inset.

with the commercial laser stabilization (specified jitter $\approx$500 kHz), the broadening of the hole spectra is too large to resolve the excited-state quadrupole coupling. The width of the resonance lines is of the order of 1 MHz in this case [Fig. 5(e)].

To resolve the full structure of the spectrum, we locked the laser to a high-finesse optical cavity (linewidth 1 MHz) using the Pound Drever locking scheme.[25] An intracavity electro-optic modulator (EOM) reduced the fast components of the frequency jitter. Under typical operating conditions, this stabilization setup reduced the laser jitter to $<$30 kHz.

Laser amplitude fluctuations and intensity changes from the frequency-dependent efficiency of the AOM's that shift the laser frequency, cause significant deteriorations of the signal. We therefore added an intensity stabilization that kept the probe beam intensity incident on the sample constant.

Hole-burning spectra were obtained by subtracting the probe signal in the presence of the pump beam from an otherwise identical scan without pump laser. To further increase the signal to noise ratio, we summed over 1000 scans.

Figure 5 shows the hole-burning spectrum obtained with the homebuilt stabilization [Fig. 5(a)] and compares it to the spectrum obtained with the commercial system [Fig. 5(e)]. Obviously the improved stabilization allows one to clearly resolve the hyperfine structure.

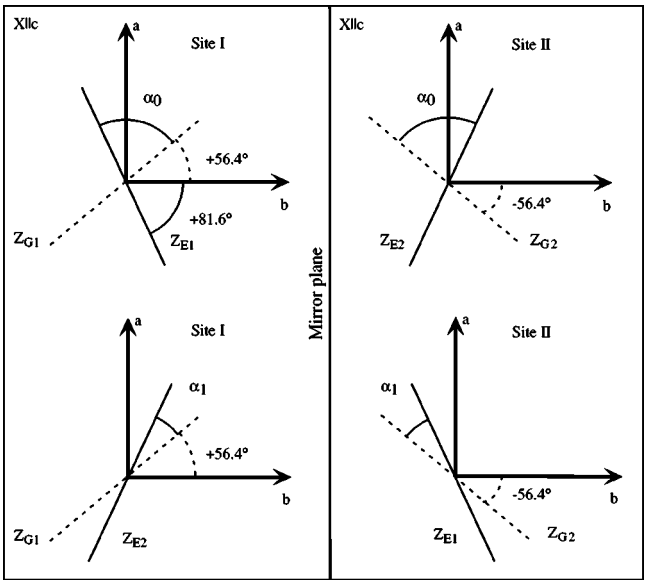

FIG. 4. Possible orientations of principal axis systems in the ground state Z_{Gi} (i=1,2) and the excited state Z_{Ei} for the two nonequivalent lattice sites (I, II) and the crystal axis system (a, b, c). The X axis of the quadrupole tensor for the ground and the excited states in both lattice sites coincide with the crystal c axis. Two assignments of the ground vs excited-state axes with different relative rotation angles indicated by α_0 and α_1 are possible.

IV. RESULTS AND DISCUSSION

A. Theoretical spectra

Our approach to the calculation of the spectra is described in Sec. II B. A number of material parameters enter the calculation, most of which have been measured independently. The relaxation rates have been measured by Blasberg.[5] At the relevant temperature of 5 K, they are $\Gamma_{5/2\leftrightarrow 3/2}=5.93\ s^{-1}$, $\Gamma_{5/2\leftrightarrow 1/2}=1.42\ s^{-1}$, $\Gamma_{3/2\leftrightarrow 1/2}=3.02\ s^{-1}$. The lineshape of the holes and antiholes depends not only on parameters of the crystal,[26] but also on the spectral properties of the laser. The experimental spectra show consistently wider lines for the antiholes than for the holes. This is consistent with the assumption that they include an additional contribution from the inhomogeneous width of the ground-state nuclear-spin transitions, which is of the order of 30–50 kHz, HWHH.[9] The widths of the resonance lines in the experimental spectrum were determined by fitting them with the Lorentzian lines. For the holes the linewidths were 63 kHz (HWHH) and for the antiholes between 120 and 160 kHz. Since the two laser fields couple to different ground-state levels when measuring antiholes, their widths include a contribution from the inhomogeneously broadened nuclear-spin transitions in the electronic ground state. For the optical dipole moment, we used the value of 10^{-34} Cm, determined by the stimulated photon echo envelope modulation.[27]

B. Orientation of principal-axis systems

An important parameter for the calculation of the spectra is the relative orientation of the principal-axis systems (PAS) in the ground and excited states, which enters the optical transition matrix elements via the overlap integral of the nuclear wave functions. Earlier experiments[9] have shown that the Z axis of the principal-axis system lies in the a-b plane of the crystal, for the electronic ground state as well as the electronically excited state. In the ground state, the angle between the Z_{PAS} and the crystal b axis is $\pm$56.4°, and in the electronically excited state $\pm$81.6°. Depending on the assignment of two orientations to the two lattice sites, this leaves two possibilities for the relative orientation of the two principal axis systems of the ground and excited states, as shown in Fig. 4. In the first assignment, shown in the upper half of the figure, the angle between the two Z axes is $\alpha_0=42°$ and for the second assignment, it becomes $\alpha_1=25.2°$.

As discussed in the introduction, different values have been published in the literature for the orientation of the PAS. We therefore calculated the corresponding spectra for the published values of $\pm$16.5°,[11] $\pm$12.8°,[9] 40–60°,[12,13] and $\pm(47\pm5)°$.[14] Figures 5(b)–5(d) compare theoretical spectra for small rotation angles ($\pm$13°, $\pm$25°) and for a large rotation angle ($\pm$42°) with the experimental spectrum [Fig. 5(a)]. While the spectrum calculated for a relative orientation of 42° agrees quite well with the experimental spectrum, the 13° spectrum is clearly incompatible with the experimental data. The main difference is that at small angles, the number of transitions with significant amplitude decreases; in the limit of identical orientation, only a single hole and six antiholes would remain. The dashed line in Fig. 5 indicates the position of an antihole that corresponds to the optical transition $|3/2\rangle\leftrightarrow|3/2\rangle$. As Fig. 2 shows, a small matrix element for this transition is a clear indication that the rotation angle must be between 40° and 55°.

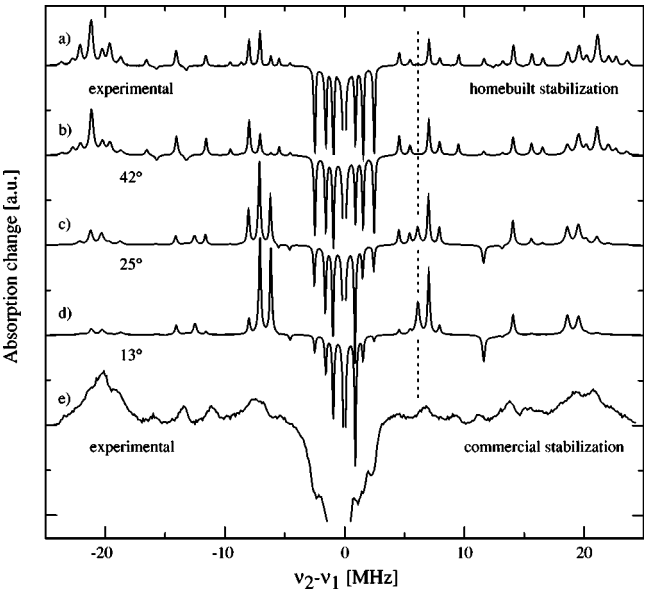

FIG. 5. Comparison of the experimental hole-burning spectrum of the 610.69-nm transition at 5 K, measured with the homebuilt and the commercial frequency stabilization, with theoretical spectra for rotation angles of 42°, 25°, and 13°. The dashed line emphasizes the position of an antihole that belongs to the $|3/2\rangle \leftrightarrow |3/2\rangle$ transition. For clarity the main hole at 0 MHz has been truncated in the spectra.

Figure 6 shows a quantitative comparison of the experimental and theoretical hole-burning spectra as a function of the orientation of the PAS. The area of the experimental and theoretical spectra has been normalized to one. The curve displays the rms deviation ξ between the experimental and theoretical spectra as a function of the rotation angle between principal-axis systems of the ground and excited states:

$$\xi = \sqrt{\sum_{i=1}^{\sharp\,\text{lines}} (A_{\text{expt.},i} - A_{\text{theor.},i})^2 \delta^2_{\text{expt.},i}} \ . \qquad (6)$$

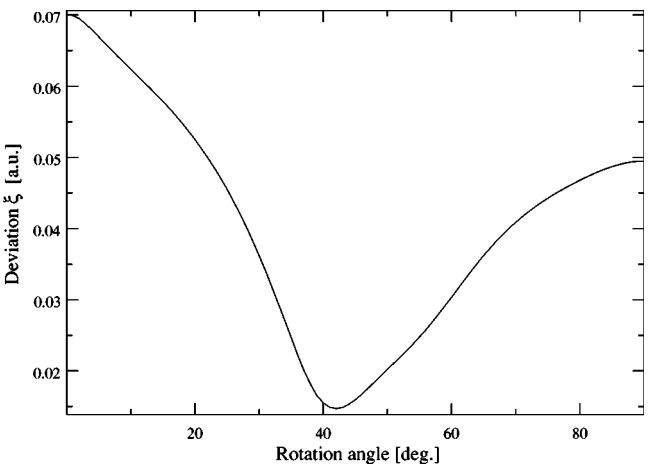

FIG. 6. Deviation of the calculated from the experimental spectrum as a function of the rotation angle between the quadrupole tensor axis of the ground and the excited states. The figure shows a minimum at 42°.

TABLE I. Absolute square of the relative matrix elements for the optical transitions connecting the $^3H_4$ ground state to the $^1D_2$ electronically excited state without external fields for a rotation angle of $\pm 42°$.

g\ e	$\lvert\pm\frac{5}{2}\rangle$	$\lvert\pm\frac{3}{2}\rangle$	$\lvert\pm\frac{1}{2}\rangle$
$\lvert\pm\frac{5}{2}\rangle$	0.469	0.319	0.212
$\lvert\pm\frac{3}{2}\rangle$	0.417	0.003	0.549
$\lvert\pm\frac{1}{2}\rangle$	0.114	0.647	0.239

The amplitudes $A_{\text{expt.}}$ and the linewidths $\delta_{\text{expt.}}$ were determined by Lorentzian fits.

The curve shows a clear minimum of $\pm 42 \pm 1°$. Table I lists the nuclear-spin contribution to the optical transition matrix elements calculated for this orientation. These values were used to calculate the theoretical spectrum for $\pm 42°$ in Fig. 5(b).

This angle is in good agreement with the value obtained by Mitsunaga through the modulation of stimulated photon echos.[13] Their numerical simulations of the modulation behavior were consistent with angles between 40° and 60°. Blasberg measured the coherent Raman beats[14] and found the best agreement for angles of $47° \pm 5°$. The smaller angles of $\pm 12.8°$, however, which were suggested by Mitsunaga[9] on the basis of the coherent Raman measurements or $\pm 16.5°$ proposed by Wokaun[11] on the basis of anticrossing experiments, are clearly excluded by these results. These latter measurements used setups in which the signal depends only on a single state, either the ground or the excited state. They are therefore only sensitive to the orientation of the individual tensors, not to the *relative* orientation of the two tensors, which remains ambiguous. In contrast to those measurements, the present setup relies on the overlap of the nuclear state functions, which is an excellent measure of the relative orientation, although it does not provide the absolute orientations. Our results are also in agreement with low-field nuclear quadrupole resonance (NQR) data,[5] where the principal-axis system was determined by measuring the NQR spectra as a function of the orientation of a weak magnetic field. In these experiments, the absolute orientation of both the PAS wasdetermined independently; however, an ambiguity remained for the assignment of the principal-axis systems to nuclear sites. As a result, two possible values were obtained for the relative orientation. The value of $\pm 42°$ obtained from this study agrees well with the larger of those values and excludes the smaller. Taking these results together, we arrive at the orientation shown in the upper part of Fig. 4.

V. CONCLUSION

In this paper we have demonstrated that the high-resolution hole-burning spectroscopy allows one to measure nuclear-spin energies in the electronically excited state as well as in the electronic ground state. Compared to other techniques, the hole-burning approach is especially sensitive to the *relative* orientation of the principal-axis systems in the

two electronic states. In the system considered here, Pr^{3+}:$YAlO_3$, we found that the angle between the two PAS is $\pm 42°$, thus resolving discrepancies in earlier measurements.[9,11,13,14] The technique should be applicable to other systems as well, where the orientation of the PAS is not fixed by symmetry.

ACKNOWLEDGMENTS

This work was supported by DFG Grant No. Su 192/4–3. The laser stabilization, which was essential for this work, was developed with extensive help from Matt Sellars (ANU Canberra).

*Present address: TOPTICA Photonics AG, Fraunhoferstrasse 14, 82152 Martinsried, Germany

[1] S. Völker, Annu. Rev. Phys. Chem. **40**, 499 (1989).
[2] M. Mitsunaga, R. Yano, and N. Uesugi, Opt. Phys. Lett. **16**, 1890 (1991).
[3] M. Mitsunaga, N. Uesugi, and K. Sugiyama, Opt. Lett. **18**, 1256 (1993).
[4] W.R. Babbitt and T.W. Mossberg, Opt. Lett. **20**, 910 (1995).
[5] T. Blasberg and D. Suter, Chem. Phys. Lett. **215**, 668 (1993).
[6] R.M. Macfarlane and G. Wittmann, Opt. Lett. **21**, 1289 (1996).
[7] G. Wittmann and R.M. Macfarlane, Opt. Lett. **21**, 426 (1996).
[8] R.L. Cone, R.T. Harley, and M.J.M. Leask, J. Phys. C **17**, 3101 (1984).
[9] M. Mitsunaga, E.S. Kintzer, and R.G. Brewer, Phys. Rev. B **31**, 6947 (1985).
[10] R.M. MacFarlane and R.M. Shelby, in *Spectroscopy of Solids Containing Rare Earth Ions*, edited by A. Kaplyanskii and R. M. MacFarlane (North-Holland, Amsterdam, 1987).
[11] A. Wokaun, S.C. Rand, R.G. DeVoe, and R.G. Brewer, Phys. Rev. B **23**, 5733 (1981).
[12] M. Mitsunaga, Phys. Rev. A **42**, 1617 (1990).
[13] M. Mitsunaga, R. Yano, and N. Uesugi, Phys. Rev. B **45**, 12 760 (1992).
[14] T. Blasberg and D. Suter, Opt. Commun. **120**, 55 (1995).
[15] S. Hüfner, *Optical Spectra of Transparent Rare Earth Compounds* (Academic Press, New York, 1978).
[16] B. Bleaney, Physica (Utrecht) **69**, 317 (1973).
[17] A. Abragam and B. Bleaney, *EPR of Transition Ions* (Clarendon, Oxford, 1970).
[18] M.H. Cohen and F. Reif, Solid State Physics **5**, 321 (1957).
[19] M.A. Teplov, Sov. Phys. JETP **26**, 872 (1968).
[20] T. Blasberg and D. Suter, Phys. Rev. B **48**, 9524 (1993).
[21] L.E. Erickson, Phys. Rev. B **19**, 4412 (1979).
[22] L.E. Erickson, Phys. Rev. B **24**, 5388 (1981).
[23] L.E. Erickson, Phys. Rev. B **16**, 4731 (1977).
[24] R. Diehl and G. Brandt, Mater. Res. Bull. **10**, 85 (1975).
[25] R.W.P. Drever, J.L. Hall, F.V. Kowalski, J. Hough, G.H. Ford, A.J. Munley, and H. Ward, Appl. Phys. B: Photophys. Laser Chem. **31**, 97 (1983).
[26] R.M. Macfarlane, J. Lumin. **100**, 1 (2002).
[27] S. Glaser, G. Wäckerle and K.P. Dinse, Chem. Phys. Lett. **121**, 267 (1985).